NANO LETTERS

2007
Vol. 7, No. 6
1799−1803

Lateral Self-Aligned p-Type In_2O_3 Nanowire Arrays Epitaxially Grown on Si Substrates

C. L. Hsin,[†,‡] J. H. He,[†] C. Y. Lee,[†] W. W. Wu,[†] P. H. Yeh,[†] L. J. Chen,*[,†] and Z. L. Wang*[,‡]

Department of Materials Science and Engineering, National Tsing Hua University, Hsinchu, Taiwan, Republic of China, and School of Materials Science and Engineering, Georgia Institute of Technology, Atlanta, Georgia 30332-0245

Received April 3, 2007; Revised Manuscript Received May 4, 2007

ABSTRACT

Lateral orientated growth of In_2O_3 nanowire (NW) and nanorod (NR) arrays has been achieved by a vapor transport and condensation method on (001) and (111) surfaces of Si substrates. The single crystalline In_2O_3 NWs and NRs were grown along $[2\bar{1}\bar{1}]$ in parallel to the Si $\pm[1\bar{1}0]$ and lying in the substrate plane. The electrical measurements show that the In_2O_3 NWs are p-type semiconductor. By N^+ doping, the resistivity of the In_2O_3 NWs has been tuned. The lateral self-aligned In_2O_3 NW and NR arrays on Si can offer some unique advantages for fabricating parallel nanodevices that can be integrated directly with silicon technology.

Nanostructured materials have attracted much attention because of their novel properties that may lead to the basic understanding and novel applications. A large number of nanostructures have been fabricated using various methods.[1−7] Intensive efforts have been directed to the functional metal oxides for possible applications in nanotechnologies.[8−11] Synthesis, analysis of the structures and characterization of the properties of these metal oxides nanomaterials have been well documented.[12−16]

In_2O_3 is a wide band gap oxide based semiconductor. It is an important material that has applications in optoelectronic devices and sensors for gas and biological sensing.[17−20] There has been a great deal of research on synthesis and characterization of nanostructured In_2O_3.[21−24] Among these nanostructures, nanowire (NW) stands out as one of the most important and their electrical properties have been widely studied.[25−27] However, it was difficult to fabricate the NW devices since the In_2O_3 NWs reported previously were mostly oriented randomly on the substrate surface. The most useful NWs are likely to be the ones that are oriented in arrays perpendicular or parallel to the substrates. Although there are techniques available for aligning the NWs after the growth, such as nanoimprint, Langmuir−Blodgett growth, and electric-field assisted assembly technique, additional effort is still needed for many applications.[28−30] In this Letter, we report the epitaxial growth of lateral self-aligned In_2O_3 NW and nanorod (NR) arrays on Si substrates by a vapor transport and condensation method. These NWs show high directional regularity and correlation with the Si substrate. The properties of the NWs can be changed and modulated by nitrogen doping. A simple two-probe method was used to measure the electrical transport properties of the NW.

Single crystal, 1−30 Ω cm, (001) and (111) oriented silicon wafers were used as substrates. A 1-nm-thick Ag or Au film was deposited on the Si substrates under a pressure of 6×10^{-6} Torr in an electron beam evaporation system. Prior to the loading into the system, the wafer was cleaned by standard RCA process. A vacuum furnace with vacuum better than 10^{-2} Torr was used to grow the nanostructures. The Ar and O_2 were flowed through the system at the rates of 100 and 10 sccm, respectively. During the growth process, the samples were placed downstream and the In_2O_3 powder mechanically mixed with graphite at a 4:1 weight ratio was positioned upstream. The vapor source was transported and carried by the carrier gas and then condensed on the substrates. The source and samples were heated to 800−900 and 600−700 °C, respectively. With the growth temperature increased from 600 to 700 °C, the diameter of the NWs became broader and formed NRs. The diameter of the NWs was found to increase with the length. If the gas pressure was high, the NWs changed morphology to NRs or nanoparticles. If the pressure was lower than 6.3 Torr at 600 °C, no NWs were grown. By optimization of the growth temperature and pressure, NWs and NRs with various aspect ratios have been synthesized.

* Corresponding authors. E-mail: ljchen@mx.nthu.edu.tw (L.J.C.); zhong.wang@mse.gatech.edu (Z.L.W.).
[†] National Tsing Hua University.
[‡] Georgia Institute of Technology.

10.1021/nl0707914 CCC: $37.00
Published on Web 05/22/2007

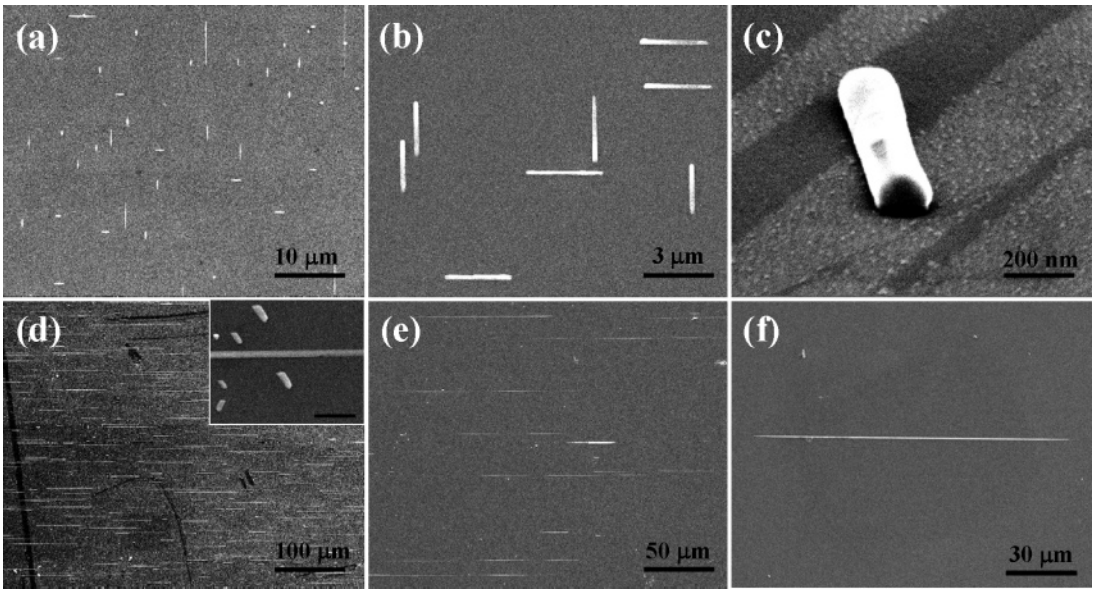

Figure 1. SEM images of the as-grown In_2O_3 NWs on silicon substrate: (a) high-magnification image of an In_2O_3 NW grown on (001) Si substrate; (b) high-magnification image of the In_2O_3 NRs on (001) Si substrate; (c) with 25° tilting SEM image of a NR; (d) low-magnification image of an In_2O_3 NW grown on (111) Si substrate (inset shows high-magnification image and the scale bar stands for 2 μm); (e) image of In_2O_3 NWs grown on (111) Si substrate with one growth direction; (f) a long In_2O_3 NW grown on (111) Si substrate.

A field emission scanning electron microscope (FESEM) was used to examine the growth products, and a JEOL-2010 transmission electron microscope (TEM) was used to investigate the microstructures and to determine the compositions of the samples. HP-4156A and Keithley 4200 were used in the electrical measurements.

Figure 1a shows an SEM image of the NW array on the (001) Si substrate synthesized at 600 °C and 6.7 Torr. The NWs were several micrometers in length. There were still some NRs formed on the substrate. As seen in Figure 1a, both NWs and NRs show the orientation ordered growth along orthogonal directions. Figure 1b shows a low-magnification SEM image of the NR array, which was synthesized at 700 °C and 7.1 Torr. The length-to-width ratio of the NRs is about 20. As seen from the cross section SEM image with a 25°-tilted angle of the NR in Figure 1b, Figure 1c shows the width of the NR is about 150 nm and the interface between the NR and the substrate is rather flat.

NWs and NRs could be grown on the substrate coated with Ag and Au. Under the same growth conditions but without metal catalyst, the yield is relatively low. Only a few NRs could be formed. In_2O_3 particles were grown on the substrates. The In_2O_3 particles still have square shape. On the (111) Si substrates, NWs would grow along three directions. NWs grown along one of these directions would be longer especially but shorter along the other two directions. Figure 1d is a low-magnification SEM image of NWs and the inset shows 60° inclined angle for NWs. If we manipulated the directions of the Si substrates and growth conditions, we could decrease the population of the short rods. Figure 1e shows that NWs can be grown along only one direction, and the lengths of the NWs are about 30−100 μm. When the source and samples temperatures were controlled at 800 and 700 °C at 7 Torr, respectively, the In_2O_3 NWs were more than 100 μm, as shown in Figure 1f. The width of the NWs is about 150−600 nm.

On the (001) Si substrate, the NW and NR arrays are aligned along two perpendicular directions. In order to investigate the orientation relationship with the Si substrate, planar view TEM images were prepared by thinning the specimen from the substrate side, so that the final specimen is a very thin Si foil with the NWs and NRs located at the top surface. Figure 2a is a TEM image of the NW and NR grown on a (001) Si substrate. Analysis of the corresponding electron diffraction pattern, which is dominated by the diffraction from Si, as shown in the inset, indicates that the NWs grew along the ⟨110⟩ directions of Si.

To study the interface between the NWs and NDs with the substrate, cross-section TEM samples were prepared. Figure 2b is TEM cross-sectional image of the NW located at the top of the Si substrate, in which the direction of the incident electron beam is along Si $[01\bar{1}]$, in parallel to the growth direction of the NW. The NW had a semiellipsoidal cross section. The height of the NW is about two-fifths of the width. A thin SiO_2 layer about 10 nm can be seen between the NW and the substrate. Figure 2c is the corresponding SAED pattern that shows the relationship between the NW and the substrate although there is a thin silica layer between the two. The upward direction of the NW is determined to be [111], and the growth direction is $[2\bar{1}\bar{1}]$. Figure 2d is a HRTEM image of the NW after filtering the noise, clearly indicating the crystalline structure of the NW.

Figure 3 shows that NWs grew along $\langle 1\bar{1}0\rangle$ directions on (111) Si substrate. On analysis of the diffraction pattern in the inset of Figure 3, In_2O_3 NWs are parallel to Si $\langle 1\bar{1}0\rangle$ directions, which coincides with the results in Figure 2a.

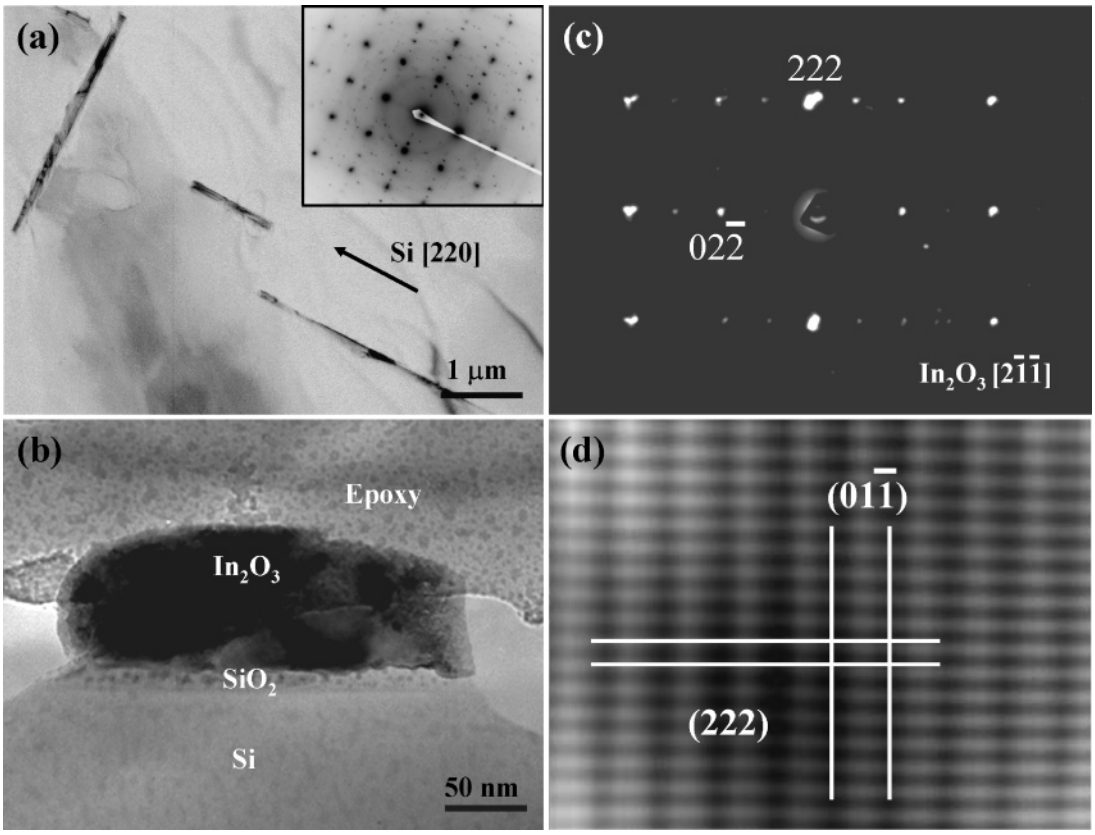

Figure 2. (a) Planar view of TEM image of the In_2O_3 NWs grown epitaxially on (001) Si. Inset shows the corresponding SAED pattern. The normal direction is Si [001]. (b) Cross section TEM image of an In_2O_3 NW on the Si substrate. (c) SAED pattern of the NW. (d) HRTEM image of the NW after filtering noise.

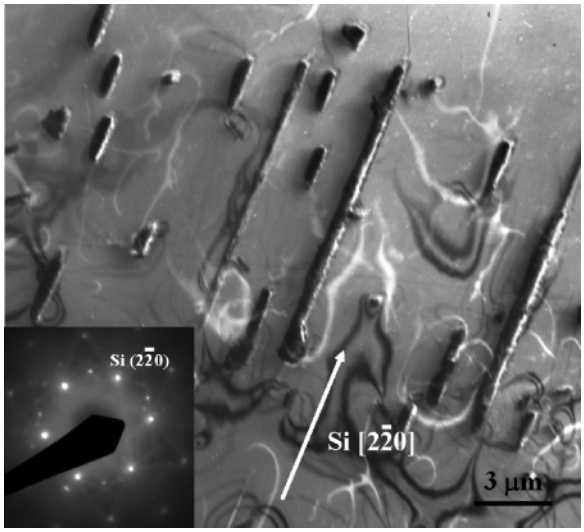

Figure 3. TEM image of the In_2O_3 NWs grown on (111) Si. Inset shows the corresponding SAED pattern, the normal direction is Si [111] and growth direction of the NWs is parallel to Si [1$\bar{1}$0].

These TEM images and diffraction patterns indicate that the growth direction of the NWs is parallel to Si ⟨1$\bar{1}$0⟩ for all Si Substrates

For the growth of the In_2O_3 NWs, In_2O_3 powder reacted with carbon to produce indium vapor at high temperature. The indium vapor is carried by Ar and condenses on the sample surface. During the growth process, the silver film agglomerated to form islands upon heating. With the exposure of O_2, the exposed Si was oxidized to form the SiO_2 layer, but the Ag islands slow down the oxidation process of the Si below the Ag islands. Some of these sites became nucleation sites when indium vapor dissolved and segregated, then forming the indium oxide. When the indium oxide NWs were formed, it is possible to match the Si lattice to form NWs along the Si [1$\bar{1}$0] direction with the [2$\bar{1}\bar{1}$] direction of the NWs as seen from Figure 2. The NWs grow longer from the nucleated indium oxides. After the In_2O_3 NWs were formed, the Si beneath the islands was oxidized, showing amorphous silica. Similar results have been reported by others.[31] The SiO_2 layer serves as the gate oxide, as seen in Figure 2b. Samples with 100 nm of SiO_2 at the surface were also used to grow the NWs under the same growth procedure. There were no NWs grown on the oxide surface. If the sample was treated with RCA cleaning procedure but without the deposition of the Au and Ag film, only a few NWs and NRs could be found, indicating the catalytic effect of the Ag was important for the growth.

The lattice mismatch between In_2O_3 (2$\bar{1}\bar{1}$) and Si (1$\bar{1}$0) was about 7%. There have been reports that the growth layer below the critical thickness would still form epitaxially even at a large mismatch with the substrate.[32] In previous reports, InAs/InP hetrostructured NWs with 6% lattice mismatch have been grown.[33] In the beginning, the In_2O_3 NWs were thin enough to match Si at large mismatch. After the SiO_2 interlayer formed, the NWs grow longer from the nucleated indium oxides.

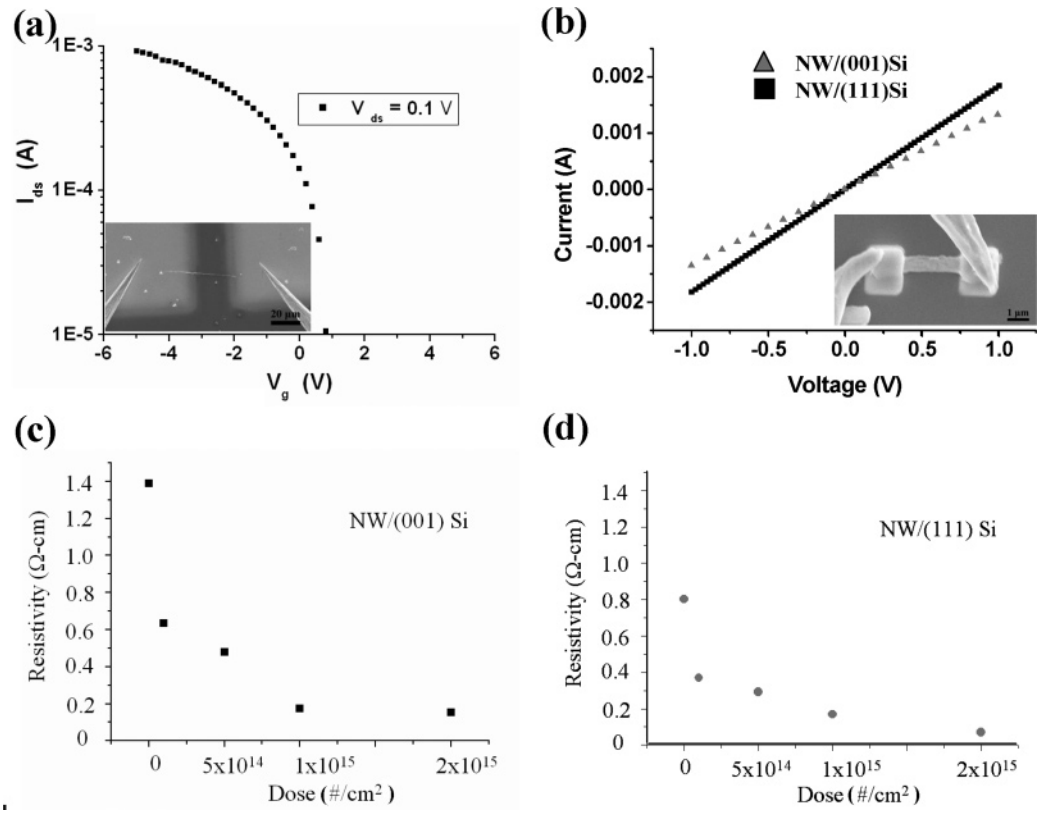

Figure 4. Electrical properties of single NWs. Room temperature. (a) Current vs gate voltage curve with source−drain voltage $V_{ds} = 0.1$ V. Insets in (a) and (b) show the SEM image of the fabricated device on (111) and (001) Si substrates, respectively. (b) Current vs drain voltage curve of the single NWs grown on (001) and (111) Si with gate voltage $V_g = 0$ V, respectively. (c, d) Resistivity of the NWs grown on (001) and (111) Si, respectively, as a function of the doping dose of nitrogen.

The electrical properties of the NWs have been characterized by two-electrode transport measurements. Since the NWs are self-aligned on the (111) Si substrate with several tens of micrometers in length, it is possible to fabricate a metal electrode on the NW without using electron beam lithography. A 200-mesh Cu grid was used as a mask when the NWs were long enough. A Cu grid was positioned on an appropriate place so that a grid line crosses one NW with the ends of the NW sticking out. One hundred nanometers of Pt was deposited as the contact metal. After deposition, the copper mesh was detached using a tweezers and the sample was annealed at 300 °C in a vacuum furnace under 10^{-2} Torr. Another way to form the metal pads is to use the FIB system. For NWs grown on the (001) Si substrate, Pt was deposited at the two ends of the NWs. The pads are 1.5 μm square. The silicon oxide at the interface was used as gate oxide, and Si substrate was used as a back gate of the device. The device was measured at room temperature with a HP-4156A and Keithley 4200 at atmosphere pressure and vacuum, respectively. The Keithley 4200 was equipped with a four-probe FESEM and vacuum pressure was lower than 10^{-3} Pa. Figure 4a shows the $I_{ds}-V_g$ curve at $V_{ds} = 0.1$ V at atmospheric pressure. The $I-V$ curve shows that the NW is a p-type semiconductor. This is the first time for reporting p-type semiconducting In_2O_3 NWs. This is the first observation of p-type In_2O_3 NWs. According to previous studies, the growth of n-type NWs was attributed to the presence of oxygen vacancy defects. The p-type semiconducting is likely due to the indium vacancies, which contribute the holes in the NWs.

Figure 4b shows the $I_{ds}-V_{ds}$ curve of NWs grown on (001) and (111) Si substrates with $V_g = 0$ V, respectively. The devices were measured in vacuum at zero bias, and the resistivity was estimated to be 3292 and 1092 $\mu\Omega$ cm, respectively, for the NWs grown on (001) and (111) Si substrates. The difference in resistivity is contributed to the defect concentration of the NWs, which implies the defect concentration is higher in the NWs grown on the (111) Si substrate than that on (001). From the $I_{ds}-V_{ds}$ curve, there is no Schottky barrier at the metal/semiconductor interface. Insets in parts a and b of Figure 4 show the SEM image of the probes and the fabricated device.

The electrical properties of the NWs were tuned by doping with nitrogen. The as-grown samples were implanted with N^+ by ion implantation at 20 kV, followed by annealing at 1000 °C for 30 min at 10^{-2} Torr. Parts c and d of Figure 4 show the resistivity data of nitrogen-doped NWs grown on (001) and (111) Si substrate with $V_g = 0$ V, respectively, for the NWs doped using different doses. The resistivity of the as-annealed NWs was calculated, and it was high enough to be considered as an insulator. With the increase of N^+ implantation, the resistivity of the NWs would decrease. Because the electrical property would be changed and

manipulated, it is believed that the NW in this work would be more applicable for fabricating ultrasensitive sensors.

In summary, lateral self-aligned In_2O_3 NW and NR arrays on Si substrate were synthesized for the first time. The orientation relationships between the NWs and the substrates are $In_2O_3(111)[2\bar{1}\bar{1}]$ || Si(001)[110]. A NW transistor on the Si substrate was fabricated. By measurment of the electric property, the In_2O_3 NW was found to be p-type semiconductor. The electric conductivity of the NW was tuned by nitrogen doping. Our study shows that the lateral NWs could offer a new building block for designing and building novel nanodevices that can be integrated directly with silicon technology.

Acknowledgment. The research is supported by the Republic of China National Science Council Grant No. NSC 94-2215-E-007-018 and Ministry of Education Grant No. 91-E-FA04-1-4.

References

(1) Lieber, C. M.; Morales, A. M. *Science* **1998**, *279*, 208.
(2) Wu, Y.; Xiang, J.; Yang, C.; Lu, W.; Lieber, C. M. *Nature* **2004**, *430*, 61.
(3) Wang, Z. L.; Gao, R. P.; Gole, J. L.; Stout, J. D. *Adv. Mater.* **2000**, *12*, 1938.
(4) He, J. H.; Wu, T. H.; Hsin, C. L.; Chen, L. J.; Wang, Z. L. *Electrochem. Solid-State Lett.* **2005**, *8*, G254−G257.
(5) Wu, Y.; Cui, Y.; Huynh, L.; Barrelet, C. J.; Bell, D. C.; Lieber, C. M. *Nano Lett.* **2004**, *4*, 433.
(6) He, J. H.; Wu, T. H.; Hsin, C. L.; Li, K. M.; Chen, L. J.; Chueh, Y. L.; Chou, L. J.; Wang, Z. L. *Small* **2006**, *2*, 116.
(7) Li, Y.; Xiang, J.; Qian, F.; Gradecak, S.; Wu, Y.; Yan, H.; Blom, D. A.; Lieber, C. M. *Nano Lett.* **2006**, *6*, 1468.
(8) Huang, M. H.; Mao, S.; Feick, H.; Yan, H.; Wu, Y.; Kind, H.; Weber, E.; Russo, R.; Yang, P. D. *Science* **2001**, *292*, 1897.
(9) Pan, Z. W.; Dai, Z. R.; Wang, Z. L. *Science* **2001**, *291*, 1947.
(10) Kong, X. Y.; Ding, Y.; Yang, R.; Wang, Z. L. *Science* **2004**, *27*, 1348.
(11) Chang, K. W.; Wu, J. J. *Adv. Mater.* **2004**, *16*, 545.
(12) Chen, J.; Xu, L.; Li, W. Y.; Gou, X. L. *Adv. Mater.* **2005**, *17*, 582.
(13) Hsin, C. L.; He, J. H.; Chen, L. J. *Appl. Phys. Lett.* **2006**, *88*, 063111.
(14) Nanu. M.; Schoonman, J.; Goossens, A. *Adv. Mater.* **2004**, *16*, 453.
(15) Fan, H. J.; Scholz, R.; Zacharias, M.; Goesele, U.; Bertram, F.; Forster, D.; Christen, J. *Appl. Phys. Lett.* **2005**, *86*, 023113.
(16) Liu, Y.; Dong, J.; Liu, M. L. *Adv. Mater.* **2004**, *16*, 353.
(17) Li, C.; Lei, B.; Zhang, D. H.; Liu, X. L.; Han, S.; Tang, T.; Rouhanizadeh, M.; Hsiai, T.; Zhou, C. G. *Appl. Phys. Lett.* **2003**, *83*, 4014.
(18) Zhang, D. H.; Liu, Z. Q.; Li, C.; Tang, T.; Liu. X. L.; Han, S.; Lei, B.; Zhou, C. G. *Nano Lett.* **2004**, *4*, 1919.
(19) Li, C.; Zhang, D. H.; Liu, X. L.; Han, S.; Tang, T.; Han, J.; Zhou, C. G. *Appl. Phys. Lett.* **2003**, *82*, 1613.
(20) Li, C.; Zhang, D. H.; Lei, B.; Han, S.; Liu, X. L.; Zhou, C. G. *J. Phys. Chem. B* **2003**, *107*, 12451.
(21) Guha. P.; Kar, S.; Chaudhuri, S. *Appl. Phys. Lett.* **2004**, *85*, 3851.
(22) Nguyen, P.; Ng, H. T.; Yamada, T.; Smith, M. K.; Li, J.; Han, J.; Meyyappan, M. *Nano Lett.* **2004**, *4*, 651.
(23) Li, Y.; Bando, Y.; Golberg, D. *Adv. Mater.* **2003**, *15*, 581.
(24) Hsin, C. L.; He, J. H.; Chen, L. *J. Appl. Surf. Sci.* **2005**, *244*, 101.
(25) Liu. F.; Bao, M. Q.; Wang, K. L.; Li, C.; Lei, B.; Zhou, C. G. *Appl. Phys. Lett.* **2005**, *86*, 213101.
(26) Zhang, D. H.; Li, C.; Han, S.; Liu, X. L.; Tang, T.; Jin, W.; Zhou, C. G. *Appl. Phys. Lett.* **2003**, *82*, 112.
(27) Lei, B.; Li, C.; Zhang, D. H.; Zhou, Q. F.; Shung, K. K.; Zhou, C. G. *Appl. Phys. Lett.* **2004**, *84*, 4553.
(28) Hochbaum, A. I.; Fan, R.; He, R.; Yang, P. D. *Nano Lett.* **2005**, *5*, 457.
(29) Whang, D. M.; Jin. S.; Wu, Y.; Lieber, C. M. *Nano Lett.* **2003**, *3*, 1255.
(30) Smith, P. A.; Nordquist, C. D.; Jackson, T. N.; Mayer, T. S. *Appl. Phys. Lett.* **2000**, *77*, 1399.
(31) Cerutti, L.; Ristic, J.; Fernandez-Garrido, S.; Calleja, E.; Trampert, A.; Ploog, K. H.; Lazic, S.; Calleja, J. M. *Appl. Phys. Lett.* **2006**, *88*, 213114.
(32) Zhang, T. Y.; Su, Y. J. *Appl. Phys. Lett.* **1999**, *74*, 1689.
(33) Bjork, M. T.; Ohlsson, B. J.; Sass, T.; Persson, A. I.; Thelander, C.; Magnusson, M. H.; Deppert, K.; Wallenberg, L. R.; Samuelson, L. *Appl. Phys. Lett.* **2002**, *80*, 1058.

NL0707914